Constraints on cosmic strings using data from the third Advanced LIGO–Virgo observing run - Supplemental Material

The LIGO Scientific Collaboration, the Virgo Collaboration and the KAGRA Collaboration

I. SUPPLEMENTAL MATERIAL

A. Table of quantities appearing in the paper

The main quantities used in this analysis and their meaning are listed in Table I A.

B. Loop distributions

For model **A**, the loop distribution is given by the sum of

$$t^4\frac{\mathrm{d}^2\mathcal{N}}{\mathrm{d}\ell\mathrm{d}V}_{\mathrm{rad}} = \frac{0.18\times 2\sqrt{\mathrm{H}_0}\Omega_{\mathrm{rad}}{}^{3/4}}{(\gamma+\gamma_{\mathrm{d}})^{5/2}}t^{3/2}(1+z)^3 \times\begin{cases}\Theta\left(0.18t-\ell\right) & t<t_{\mathrm{eq}}\\ \Theta\left[0.18t_{\mathrm{eq}}-\ell+\gamma_{\mathrm{d}}(t-t_{\mathrm{eq}})\right] & t>t_{\mathrm{eq}}\end{cases} \quad (1)$$

for loops produced during the radiation era, and

$$t^4\frac{\mathrm{d}^2\mathcal{N}}{\mathrm{d}\ell\mathrm{d}V}_{\mathrm{mat}} = \frac{0.27-0.45\gamma^{0.31}}{(\gamma+\gamma_{\mathrm{d}})^2}\Theta(0.18-\gamma) \times\Theta\left[\ell+\gamma_{\mathrm{d}}(t-t_{\mathrm{eq}})-0.18t_{\mathrm{eq}}\right] \quad (2)$$

for loops produced during the matter era. Note that t_{eq} is the time of the radiation to matter transition and that $\gamma_{\mathrm{d}}=\Gamma_{\mathrm{d}}G\mu$.

Models **B** and **C** rely on the assumption that loops are produced at all sizes with a given power-law. The loop production $\mathcal{P}$ is parametrized by two additional parameters (c,χ)

$$t^5\mathcal{P} = c\left(\frac{\ell}{t}\right)^{2\chi-3}, \quad (3)$$

and is cutoff on scales smaller than the gravitational backreaction scale $\gamma_{\mathrm{c}}\approx 20(G\mu)^{1+2\chi}$. The parameter χ controls the *tilt* of the loop production function, low values of χ favor the production of very small loops whereas high values of χ can be approximated by a Dirac delta loop production function on the large scales, i.e., to the one-scale model. For model **B**, the loop distribution is the sum of

$$t^4\frac{\mathrm{d}^2\mathcal{N}}{\mathrm{d}\ell\mathrm{d}V}_{\mathrm{rad}} = \begin{cases}\dfrac{0.08}{(\gamma+\gamma_{\mathrm{d}})^{3-2\chi_{\mathrm{rad}}}} & \gamma_{\mathrm{d}}<\gamma\\ \dfrac{0.08(1/2-2\chi_{\mathrm{rad}})}{(2-2\chi_{\mathrm{rad}})\gamma_{\mathrm{d}}\gamma^{2-2\chi_{\mathrm{rad}}}} & \gamma_{\mathrm{c}}<\gamma<\gamma_{\mathrm{d}}\\ \dfrac{0.08(1/2-2\chi_{\mathrm{rad}})}{(2-2\chi_{\mathrm{rad}})\gamma_{\mathrm{d}}\gamma_{\mathrm{c}}^{2-2\chi_{\mathrm{rad}}}} & \gamma<\gamma_{\mathrm{c}}\end{cases} \quad (4)$$

for loops produced during the radiation era,

$$t^4\frac{\mathrm{d}^2\mathcal{N}}{\mathrm{d}\ell\mathrm{d}V}_{\mathrm{mat}} = \begin{cases}\dfrac{0.015}{(\gamma+\gamma_{\mathrm{d}})^{3-2\chi_{\mathrm{mat}}}} & \gamma_{\mathrm{d}}<\gamma\\ \dfrac{0.015(1-2\chi_{\mathrm{mat}})}{(2-2\chi_{\mathrm{mat}})\gamma_{\mathrm{d}}\gamma^{2-2\chi_{\mathrm{mat}}}} & \gamma_{\mathrm{c}}<\gamma<\gamma_{\mathrm{d}}\\ \dfrac{0.015(1-2\chi_{\mathrm{mat}})}{(2-2\chi_{\mathrm{mat}})\gamma_{\mathrm{d}}\gamma_{\mathrm{c}}^{2-2\chi_{\mathrm{mat}}}} & \gamma<\gamma_{\mathrm{c}}\end{cases} \quad (5)$$

for loops produced during the matter era, and

$$t^4\frac{\mathrm{d}^2\mathcal{N}}{\mathrm{d}\ell\mathrm{d}V}_{\mathrm{rad-mat}} = \left(\frac{t}{t_{\mathrm{eq}}}\right)^3\left(\frac{1+z}{1+z_{\mathrm{eq}}}\right)^3 t_{\mathrm{eq}}^4 \times\frac{\mathrm{d}^2\mathcal{N}}{\mathrm{d}\ell\mathrm{d}V}^{(3)}_{\mathrm{rad}}\left[\frac{\gamma t+\gamma_{\mathrm{d}}(t-t_{\mathrm{eq}})}{t_{\mathrm{eq}}}\right] \quad (6)$$

for loops produced during the radiation era and decaying during the matter era. The subscripts $_{\mathrm{rad}}$ and $_{\mathrm{mat}}$ refer to the radiation- and matter-dominated eras, respectively, and γ_{c} is the gravitational back-reaction scale.

For model **C**, the loop distribution can be approximated in the radiation era as

$$t^4\frac{\mathrm{d}^2\mathcal{N}}{\mathrm{d}\ell\mathrm{d}V}_{\mathrm{rad}} = \frac{c_{\mathrm{rad}}}{1/2-2\chi_{\mathrm{rad}}} \times\begin{cases}(\gamma+\gamma_{\mathrm{d}})^{2\chi_{\mathrm{rad}}-3}-\dfrac{\gamma_\infty^{2\chi_{\mathrm{rad}}-1/2}}{(\gamma+\gamma_{\mathrm{d}})^{5/2}} & \gamma_{\mathrm{d}}<\gamma\\ \dfrac{\gamma^{2\chi_{\mathrm{rad}}-2}}{(2-2\chi_{\mathrm{rad}})\gamma_{\mathrm{d}}}-\dfrac{\gamma_\infty^{2\chi_{\mathrm{rad}}-1/2}}{(\gamma+\gamma_{\mathrm{d}})^{5/2}} & \gamma_{\mathrm{c}}<\gamma<\gamma_{\mathrm{d}}\\ \dfrac{\gamma_{\mathrm{c}}^{2\chi_{\mathrm{rad}}-2}}{(2-2\chi_{\mathrm{rad}})\gamma_{\mathrm{d}}}-\dfrac{\gamma_\infty^{2\chi_{\mathrm{rad}}-1/2}}{(\gamma+\gamma_{\mathrm{d}})^{5/2}} & \gamma<\gamma_{\mathrm{c}}\end{cases} \quad (7)$$

and in the matter era as

$$t^4\frac{\mathrm{d}^2\mathcal{N}}{\mathrm{d}\ell\mathrm{d}V}_{\mathrm{mat}} = \frac{c_{\mathrm{mat}}}{1-2\chi_{\mathrm{mat}}} \times\begin{cases}(\gamma+\gamma_{\mathrm{d}})^{2\chi_{\mathrm{mat}}-3}-\dfrac{\gamma_\infty^{2\chi_{\mathrm{mat}}-1}}{(\gamma+\gamma_{\mathrm{d}})^{2}} & \gamma_{\mathrm{d}}<\gamma\\ \dfrac{\gamma^{2\chi_{\mathrm{mat}}-2}}{(2-2\chi_{\mathrm{mat}})\gamma_{\mathrm{d}}}-\dfrac{\gamma_\infty^{2\chi_{\mathrm{mat}}-1}}{(\gamma+\gamma_{\mathrm{d}})^{2}} & \gamma_{\mathrm{c}}<\gamma<\gamma_{\mathrm{d}}\\ \dfrac{\gamma_{\mathrm{c}}^{2\chi_{\mathrm{mat}}-2}}{(2-2\chi_{\mathrm{mat}})\gamma_{\mathrm{d}}}-\dfrac{\gamma_\infty^{2\chi_{\mathrm{mat}}-1}}{(\gamma+\gamma_{\mathrm{d}})^{2}} & \gamma<\gamma_{\mathrm{c}}\end{cases} \quad (8)$$

where γ_∞ is the size of the largest loops in scaling units.

C. The burst analysis pipeline

The cosmic string burst search pipeline is divided into three main analysis steps. First, the cosmic string gravitational waveform is searched in LIGO and Virgo data

G	Gravitational constant
z	redshift
μ	string tension
$N_{\rm c}$	average number of cusps per loop oscillation
$N_{\rm k}$	number of kinks
$\Gamma_{\rm d}$	dimensionless decay constant of cosmic strings
g_1, g_2	dimensionless prefactors for the GW amplitude and beaming angle
ℓ	cosmic string loop length
$\gamma \equiv \ell/t$	loop size parameter
θ_m	beaming angle for GW emission
$P_{\rm gw}$	power of GW emission of cosmic strings
R_i	GW burst rate
$n(\ell, t)$	number density of cosmic string loops with length ℓ at t
$\Omega_{\rm GW}(f)$	present fractional GW energy density spectrum
$\mathcal{L}$	likelihood used in the Bayesian analysis
$p(\text{parameters}\|I)$	probability density distribution of "parameters" given prior information "I"

TABLE I. Table of quantities appearing in the paper.

using match-filtering techniques. A bank of waveform templates is chosen to match the expected signal in the frequency domain:

$$\tau_{i,j}(f) = Af^{-q_i}\Theta(f_j - f)\Theta(f - f_l). \tag{9}$$

The spectral index q_i is taken from Eq. (1) of the PRL for cusps, kinks or kink-kink collisions. The waveform frequency f is limited in range using the Heaviside function Θ. The low-frequency cut-off f_l, resulting from the size of the feature producing the gravitational waves, takes values well below the sensitive band of the LIGO and Virgo detectors. We take $f_l = 16\,\mathrm{Hz}$. The high-frequency cut-off f_j is a consequence of the gravitational-wave emission being observable only within a (frequency-dependent) viewing angle θ_m, given in Eq. (3) of the PRL. The angle between the line of sight and the gravitational-wave direction, θ, must be smaller than $\theta_m/2$, yielding $f < [2g_2\ell(1+z)\theta^3]^{-1}$. This high-frequency cutoff is unknown and is considered as a free parameter, taking discrete values indexed by j. When searching for gravitational waves produced by cusps and kinks, we use 31 templates with high-frequency cutoff values distributed between 30 Hz and 4096 Hz and spaced in such a way that we guarantee less than 0.1 % loss in the signal-to-noise ratio due to template mismatch. The cutoffs f_j are sparser at higher frequencies, with 17 templates below 100 Hz. For kink-kink collisions, the gravitational-wave radiation is isotropic and a single template covering the entire frequency band is used.

The standard matched filter output for template $\tau_{i,j}$ on the gravitational wave data h_{det} is

$$\rho_{i,j,\mathrm{det}}(t) = 4\Re\int_0^\infty \frac{\tau^*_{i,j}(f)h_{\mathrm{det}}(f)}{S_n(f)}\exp(2\sqrt{-1}\pi f t)\mathrm{d}f. \tag{10}$$

Here, $S_n(f)$ is the single-sided noise power spectral density of the detector. It is estimated locally over a few minutes of detector data. The normalization parameter A in each template is determined by [1]

$$4\Re\int_0^\infty \frac{\tau^*_{i,j}(f)\tau_{i,j}(f)}{S_n(f)}\exp(2\sqrt{-1}\pi f t)\mathrm{d}f = 1. \tag{11}$$

The O3 LIGO–Virgo dataset is analyzed in five consecutive chunks of data to account for the detectors' noise evolution over the entire run. This is because the statistic we use to rank events better separates the signal from noise when the characteristics of the noise are relatively unchanged. The chunk boundaries are defined by sudden changes of sensitivity of one detector and by commissioning interventions, including the 1-month commissioning break in October 2019. The signal-to-noise ratio time-series $\rho_{i,j,\mathrm{det}}(t)$ is computed for each detector, accumulating a total of 245 days, 252 days and 250 days for the L1, H1 and V1 detectors respectively. The signal-to-noise ratio time-series are required to be above 3.75 and are clustered among templates. If multiple templates trigger within a 0.1 second window, we cluster the event as a single trigger, the parameters of which are derived from the highest signal-to-noise ratio template in the cluster.

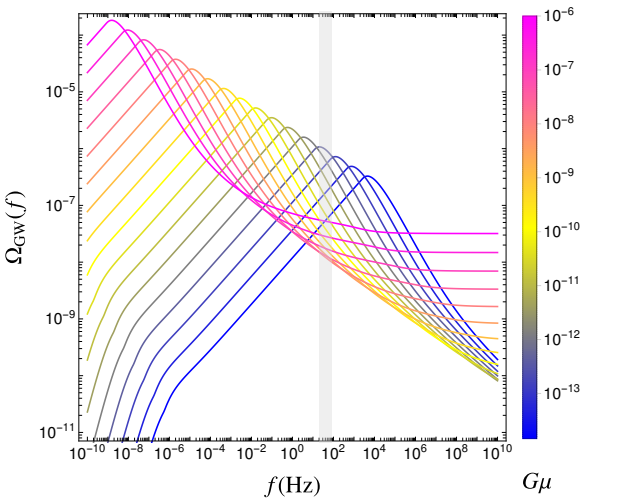

FIG. 1. The gravitational-wave spectra for model **C-1** for different choices of $G\mu$ where N_k is fixed to be 90. The gray band corresponds to the frequency range $(20-86)$ Hz used in the analysis.

After the match-filtering step, a time coincidence is performed pair-wise between the triggers of each detector using a time window wide enough to account for the maximum light-travel time between detectors and calibration time uncertainties of 8ms. A resulting set of double- and triple-coincident events is obtained when at least two detectors are taking data in nominal conditions, yielding a total observation time of $T_{\mathrm{obs}} = 273.5$ days.

Finally, to discriminate astrophysical signals from background noise, we apply the multivariate method described in [2], which uses a set of simulated cosmic string events and typical noise events to statistically infer the probability for a coincident event to be signal or noise. Hence, a likelihood ratio, Λ, is constructed with parameters characterizing the event [3]. For the O3 analysis, we introduce for the first time the event duration as a new discriminating variable. The event duration is defined as the duration for which $\rho_{i,j,\mathrm{det}}(t)$ remains above threshold considering all templates j and using a tolerance of 100 ms. Using this parameter, coupled to the signal-to-noise ratio, allows us to reject a large population of long-duration and low signal-to-noise ratio transient noise events contributing to the search background.

D. Feature in SGWB constraint for Model C-1

The stochastic gravitational-wave constraint for model **C-1** has a special feature, shown in Fig. 3 of the PRL. The appearance of this notch, when $N_{\mathrm{k}} > 70$, is induced by the unique behavior of the gravitational-wave spectrum in this model. In Fig. 1 we compare the correspond-

ing spectrum for different choices of $G\mu$ with $N_{\rm k}$ fixed to be 90. The cosmic string network produces a stochastic background in a wide frequency range, while LIGO/Virgo is only sensitive to a very narrow frequency window labeled by the grey band. As $G\mu$ increases, the stochastic power spectrum within the LIGO/Virgo window does not change monotonically. This leads to a non-exclusion in a small range of $G\mu$ when $N_{\rm k} > 70$. The exact location of the notch is determined through a detailed Bayesian analysis presented in the main text.

[1] X. Siemens, J. Creighton, I. Maor, S. Ray Majumder, K. Cannon, *et al.*, Phys.Rev. **D 73**, 105001 (2006), arXiv:gr-qc/0603115 [gr-qc].

[2] K. C. Cannon, Class.Quant.Grav. **25**, 105024 (2008).

[3] J. Aasi *et al.* (Virgo, LIGO Scientific Collaboration), Phys. Rev. Lett. **112**, 131101 (2014), arXiv:1310.2384 [gr-qc].